Acta Neuropathol (1995) 90:582–591

REGULAR PAPER

Manuel J. Caceres · Charles L. Schleien
John W. Kuluz · Barry Gelman · W. Dalton Dietrich

Early endothelial damage and leukocyte accumulation in piglet brains following cardiac arrest

Received: 15 May 1995 / Revised, accepted: 4 August 1995

Abstract This study examined the early microvascular and neuronal consequences of cardiac arrest and resuscitation in piglets. We hypothesized that early morphological changes occur after cardiac arrest and reperfusion, and that these findings are partly caused by post-resuscitation hypertension. Three groups of normothermic piglets (37.5°–38.5°C) were investigated: group 1, non-ischemic time controls; group 2, piglets undergoing 8 min of cardiac arrest by ventricular fibrillation, 6 min of cardiopulmonary resuscitation (CPR) and 4 h of reperfusion; and group 3, non-ischemic hypertensive controls, receiving 6 min of CPR after only 10 s of cardiac arrest followed by 4-h survival. Immediately following resuscitation, acute hypertension occurred with peak systolic pressure equal to 197 ± 15 mm Hg usually lasting less than 10 min. In reacted vibratome sections, isolated foci of extravasated horseradish peroxidase were noted throughout the brain within surface cortical layers and around penetrating vessels in group 2. Stained plastic sections of leaky sites demonstrated variable degrees of tissue injury. While many sections were unremarkable except for luminal red blood cells and leukocytes, other specimens contained abnormal neurons, some appearing irreversibly injured. The number of vessels containing leukocytes was higher in group 2 than in controls (3.8 ± 0.6% vs 1.4 ± 0.4% of vessels, $P < 0.05$). Evidence for irreversible neuronal injury was only seen in group 2. Endothelial vacuolization was higher in groups 2 and 3 than in group 1 ($P < 0.05$). Ultrastructural examination of leaky sites identified mononuclear and polymorphonuclear leukocytes adhering to the endothelium of venules and capillaries only in group 2. The early appearance of luminal leukocytes in ischemic animals indicates that these cells may contribute to the genesis of ischemia reperfusion injury in this model. In both groups 2 and 3 endothelial cells demonstrated vacuolation and luminal discontinuities with evidence of perivascular astrocytic swelling. Widespread microvascular and neuronal damage is present as early as 4 h after cardiac arrest in infant piglets. Hypertension appears to play a role in the production of some of the endothelial changes.

Key words Reperfusion injury · Pediatrics · Cardiopulmonary resuscitation · Blood-brain barrier · Global brain ischemia

M. J. Caceres · C. L. Schleien (✉) · B. Gelman
Department of Pediatrics (R-131),
Pediatric Critical Care Medicine,
University of Miami School of Medicine,
Post Office Box 016960, Miami, FL 33101, USA
Tel.: 1-305-585-6051; Fax: 1-305-325-0293

C. L. Schleien
Department of Anesthesiology,
University of Miami School of Medicine, Miami, Florida, USA

J. W. Kuluz
Clinical Pediatrics, University of Miami School of Medicine,
Miami, Florida, USA

W. D. Dietrich
Department of Neurology,
University of Miami School of Medicine, Miami, Florida, USA

Introduction

Cardiac arrest remains a critical medical condition which is associated with a poor prognosis in both children and adults [14, 23]. A high percentage of patients who are successfully resuscitated have poor neurological recovery due to the neuronal consequences of cardiac arrest and cardiopulmonary resuscitation (CPR). In addition, increased blood-brain barrier (BBB) permeability, which has been reported 4 h after cardiac arrest induced by ventricular fibrillation in infant piglets [40], may also allow for entry of potent medications used during CPR into brain parenchyma. The entry of these drugs could change vascular tone or have direct effects on the brain itself.

The early morphological consequences of a global ischemic insult have been investigated using rodent models of transient forebrain global ischemia [12, 33]. These models lead to severe but incomplete ischemia with only mild-to-moderate reductions in local cerebral blood flow within brain stem and cerebellar structures [36]. In con-

trast, few investigations have assessed the early morphological consequences of complete ischemia such as that which occurs following cardiac arrest. Such studies are of potential importance since the morphological response of the brain to complete ischemia might differ from that reported after transient forebrain ischemia. For example, multiorgan ischemia might lead to greater degrees of white blood cell activation and their subsequent accumulation in reperfused brain. In addition, more lactic acid is produced by the body during cardiac arrest compared with that seen during forebrain ischemia [38].

Many questions remain regarding early central nervous system changes following global ischemia particularly in the large animal model. These include the presence of glial damage and early irreversible neuronal injury, integrity of the vascular endothelium and the appearance of leukocytes which may play an important role in causing secondary injury in the brain itself. Leukocytes can release toxic compounds such as oxygen free radicals and proteases and may reduce blood flow at the microcirculatory level by occluding vessels or by inducing vasoconstriction.

The purpose of this study was to determine the light and electron microscopic consequences of complete global ischemia caused by 8 min of cardiac arrest, CPR, and a 4-h period of reperfusion. In the first two groups of animals the appearance of neuronal injury, presence of luminal leukocytes, and glial swelling in experimental animals was compared with that of sham-operated animals. Because many of the piglets were hypertensive immediately after return of spontaneous circulation, we assessed the effects of hypertension on these parameters in a third group that received CPR and epinephrine without a preceding period of ischemia. We hypothesized that endothelial membrane disruption, glial swelling, and intravascular or parenchymal leukocytes would be present at this early post reperfusion time. Since acute hypertension is seen in this model, we also hypothesized that hypertension may cause some of these ultrastructural abnormalities, thus making this aspect of CPR a likely contributor to the early microvascular and neuronal damage seen in this model.

Materials and methods

Fifteen Yorkshire piglets, 2–3 weeks old (2.8–5.5 kg), were anesthetized with pentobarbital (40 mg/kg i.p.) and ventilated with a volume-cycled ventilator through an endotracheal tube secured by a tracheostomy. Fractional inspired oxygen concentration was 0.3–0.4. End-tidal CO_2 was monitored and maintained between 35 and 45 mm Hg. Rectal temperature was maintained between 37.5° and 38.5°C throughout the experiment. Additional anesthesia was provided with pentobarbital 3–4 mg/kg i.v. when the animal began to move. A total dose of 45–55 mg/kg i.v. was generally required to maintain a depth of anesthesia adequate for surgical preparation. Saline-filled catheters were placed via the femoral vein and artery into the right atrium and intrathoracic aorta, respectively. Another catheter was placed via the axillary vein into the subclavian vein for drug infusion. A 4 French bipolar pacing wire was placed via the other femoral vein into the right heart to fibrillate the heart later in the experiment. Prior to cardiac arrest (30 min after the end of surgery) the animals received heparin sulfate 1,000 units i.v. and pancuronium 0.2 mg/kg i.v.

Ventricular fibrillation was induced by passing a 60 Hz alternating current through the pacing wire in animals in groups 2 and 3. Group 1 (n = 5) served as a sham-operated time control group and received neither ventricular fibrillation nor CPR. In group 2 (n = 6), ventilation was stopped and ventricular fibrillation was continued for 8 min prior to initiating CPR. In group 3 (n = 4), CPR was begun 10 s after the onset of ventricular fibrillation to assess the effects of post-resuscitation hypertension without a prior period of cerebral ischemia. In both groups, CPR was continued for 6 min. Sternal chest compressions were performed with a pneumatic chest compressor at a ratio of five compressions per breath, synchronized with a microprocessor to a pressure-limited ventilator (Thumper, Michigan Instruments, Grand Rapids, Mich.). Compressions were performed at a rate of 100 per min with a compression duration of 30% of the total cycle time, a combination that gives maximal cerebral blood flow during CPR in piglets [7]. Compression force was set at 45–60 N to produce a cyclic sternal displacement equivalent to 20% of the anteroposterior chest diameter. Ventilation was performed with 100% oxygen concentration, as given during human CPR, at an airway pressure of 30–35 cm H_2O. After 6 min of CPR, transthoracic defibrillation was performed with a dose of 50 J. If unsuccessful, the dose was doubled. Resuscitation was usually obtained within the first two attempts. A bolus of epinephrine 10 μg/kg i.v. was given to animals in groups 2 and 3 into the right atrium at the onset of CPR followed by a continuous i.v. infusion of 4 μg/kg per min. This dose maintains cerebral perfusion pressure at levels sufficient for near normal cerebral blood flow for 20 min of CPR in piglets [6]. After defibrillation, epinephrine infusion was decreased by 50% every 3 min if the mean aortic pressure was 70 mm Hg or above. The epinephrine infusion was stopped by 30 min in all but one animal in group 2, which remained hypotensive throughout the experiment. The fraction of inspired oxygen (FIO_2) was weaned to 40% following resuscitation by 30 min in all animals. We recorded vascular pressures from the right atrium and the intrathoracic aorta and measured arterial blood gases and pH, rectal temperature, and serum glucose in all three groups of animals throughout the experiment.

To assess BBB permeability, horseradish peroxidase (HRP, molecular weight 40,000) 150 mg dissolved in 30 ml of normal saline was infused over 15 min via the right axillary vein and allowed to circulate an additional 15 min prior to perfusion-fixation of the brain in all three groups of animals. At the conclusion of the HRP infusion all piglets received an additional dose of heparin 1,000 units i.v. and pancuronium 0.2 mg/kg i.v. Both carotid arteries, which had previously been isolated, were then catheterized for perfusion-fixation of the brain. The jugular veins were isolated and transected to allow washout of blood from the brain. One liter of 0.9% saline followed by 2 l of 2% paraformaldehyde and 2.5% glutaraldehyde in a 0.1 M sodium phosphate buffer were perfused over 20 min. The brain was removed, stored in fixative for an additional 2 h, and then placed in chilled phosphate buffer until sectioning. Following hand-dissection, vibratome sections were cut (100 μm) and reacted for HRP histochemistry with diaminobenzidine [12]. Areas including somatosensory cortex, caudate nucleus, hippocampus, anterior thalamus, cerebellum, and medulla that contained either red blood cell stasis or HRP extravasation were hand-dissected for plastic embedding. Sections (1 μm thick) were taken, and stained with toluidine blue for light microscopic examination. When parenchymal changes were observed, this tissue was dissected for thin sectioning for transmission electron microscopy [12]. The investigator was blinded to the identification of the specimens of each individual animal. Vascular injury was assessed by counting individual cross-sectioned vessels for each of the six anatomical areas described above at the light microscopy level. This was done by selecting four random fields per section at high power magnification (× 40). Approximately 60–100 vessels were counted in each anatomical area per animal. The number of vessels (mean ± SEM) counted per animal was 371 ± 24, 461 ± 40, and 459 ± 16for the three groups, respectively. Vessels were examined for endothelial membrane blebs or discontinuities and for perivascular swelling. The number of vessels containing leukocytes was recorded with notations for the presence of membrane abnormali-

ties or perivascular clearing associated with the leukocytes. Each section was also assigned a score for severity of neuronal injury: 0, if all neurons were normal; 1, if any neurons displayed mild ischemic cell change (increased density); and 2, if neurons appeared shrunken and dark. The grade for each of these three types of vascular injury was calculated by dividing the number of affected vessels by the total number of vessels examined.

Repeated measurements of physiological variables were analyzed by two-way analysis of variance. If there was a significant effect of time, values were compared with the pre-arrest value by Dunnett's test. Between-group comparisons were made using Student's *t*-test. Vascular injury scores were compared by Student *t*-test between groups and one-way analysis of variance within groups for comparison of regional differences. Values are presented as mean ± SEM. $P < 0.05$ was considered statistically significant.

Results

Physiological measurements

Pre-arrest aortic and right atrial pressures were not different between groups. During CPR, mean aortic pressure in groups 2 and 3 was 44.0 ± 4.4 and 34.3 ± 3.1 mm Hg, respectively, similar to values reported previously in this model [39]. Following resuscitation, the maximum aortic systolic pressure was 197 ± 15 mm Hg in group 2 and 209 ± 8 mm Hg in group 3. The maximum pressure elevation occurred in the first 5 min in nine of the ten animals in the two groups (4.3 ± 2.6 min). The duration of hypertension was not different between groups 2 and 3, and lasted less than 10 min in all but one animal in each group, which remained hypertensive for the duration of the survival period. Mean rectal temperature was between 37.5°C and 38.5°C throughout. In preliminary studies (n = 4), we found that brain temperature was unchanged during CPR. No animals were hypoxemic during the experiment. In group 3, P_aCO_2 was slightly lower during CPR and higher 3 min after CPR compared with group 2 (Table 1). Arterial pH decreased to 7.15–7.18 after resuscitation, reflecting the degree of metabolic acidosis usually seen following cardiac arrest in piglets [39].

Morphological findings

Group 1 – Sham operation

The brains in group 1 appeared normal by light and electron microscopic examination. Sites of extravasated HRP were not seen in vibratome sections. Blood vessels appeared well perfused with no evidence of red blood cell stasis. Neurons and astrocytes were unremarkable. The luminal surface of only 0.8 ± 0.5% of vessels had endothelial blebs, 0.6 ± 0.6% of vessels had perivascular swelling and 1.4 ± 0.4% of the vessels contained intraluminal leukocytes. Ultrastructural features also appeared normal [32].

Group 2 – Cardiac arrest

At 4 h after cardiac arrest, vibratome sections contained multiple sites of extravasated HRP (Fig. 1). Light microscopic examination commonly revealed diffuse staining within surface cortical layers. Penetrating vessels also displayed HRP staining of the vessel wall. (Fig. 1 a) In other

Table 1 Physiological data. Data given as mean ± SEM

	Group	Before arrest	CPR	3 min	60 min	120 min	225 min
Aortic systolic Pressure (mm Hg)	1	101 ± 6					
	2	119 ± 12	72 ± 5**	163 ± 11**	109 ± 9	109 ± 8	109 ± 9
	3	123 ± 3	59 ± 7	139 ± 6	116 ± 10	126 ± 14	96 ± 4
Aortic diastolic Pressure (mm Hg)	1	72 ± 4					
	2	80 ± 10	30 ± 3**	113 ± 8**	80 ± 7	82 ± 9	69 ± 6
	3	84 ± 4	28 ± 3**	106 ± 5**	88 ± 7	92 ± 8	69 ± 6
Aortic mean Pressure (mm Hg)	1	88 ± 5					
	2	97 ± 11	44 ± 4**	136 ± 8**	92 ± 7	88 ± 8	78 ± 6
	3	95 ± 4	34 ± 3**	118 ± 3**	103 ± 8	107 ± 10	81 ± 5
P_aCO_2 (mm Hg)	1	29 ± 3					
	2	39 ± 2	30 ± 6	44 ± 6	35 ± 3	40 ± 6	36 ± 3
	3	39 ± 1	19 ± 2**	53 ± 3**	37 ± 3	40 ± 4	40 ± 1
pH	1	7.53 ± 0.03					
	2	7.43 ± 0.01*	7.35 ± 0.05*	7.15 ± 0.04**	7.32 ± 0.03	7.29 ± 0.07	7.30 ± 0.03
	3	7.38 ± 0.01	7.59 ± 0.04**	7.18 ± 0.02**	7.36 ± 0.04	7.37 ± 0.02	7.38 ± 0.01
Temperature (°C)	1	37.5 ± 0.3					
	2	37.9 ± 0.3	37.9 ± 0.3	37.7 ± 0.3	38.2 ± 0.2	38.4 ± 0.2	38.1 ± 0.2
	3	37.5 ± 0.1	37.9 ± 0.2	38.1 ± 0.2	38.2 ± 0.2	38.2 ± 0.4	37.8 ± 0.2

* $P < 0.05$ different from group 3
** $P < 0.5$ different from before arrest

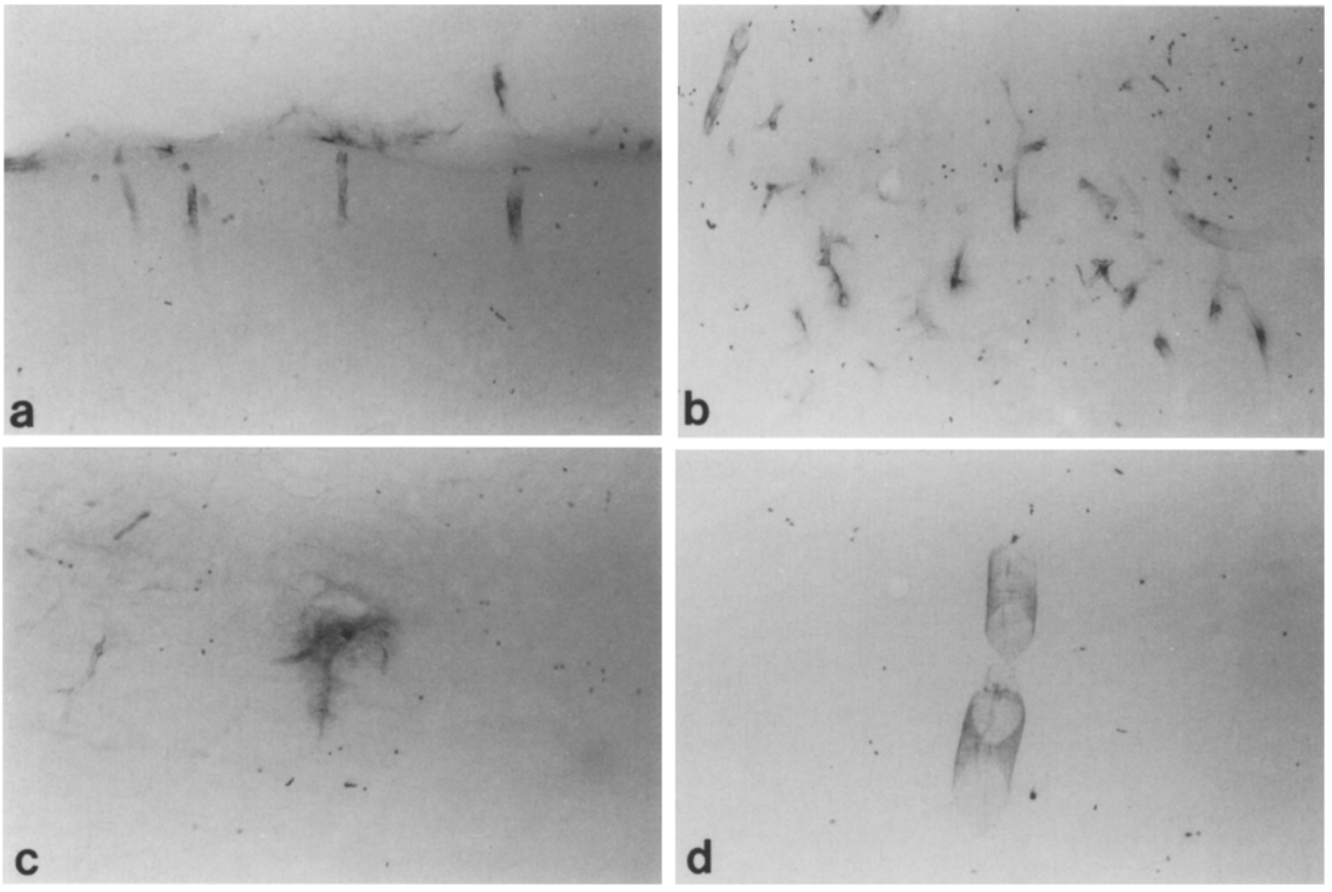

Fig. 1a–d Vibratome sections reacted for horseradish peroxidase (HRP) histochemistry. Sections taken from piglet brains 4 h after cardiac arrest. **a** Extravasated HRP is associated with several penetrating vessels within the superficial layers of somatosensory cortex. **b** Several vessels within the cerebral cortex demonstrate extravasated HRP. Evidence for red blood cell stasis is also apparent. **c** A vessel coursing within the caudate nucleus shows extravasated HRP. **d** The wall of a thalamic arteriole is outlined by HRP

regions, including the caudate nucleus, hippocampus, thalamus, cerebellum and brain stem, isolated sites of HRP leakage were seen (Fig. 1 c, d). In addition to HRP leakage, residual red blood cells were occasionally noted (Fig. 1 b), in some cases in columns indicating capillary congestion. These vascular changes were detected throughout the brain and did not appear to be restricted to any specific structure. There was, however, no apparent relationship between red cell stasis and HRP extravasation.

Plastic sections stained with toluidine blue displayed various degrees of injury (Fig. 2). In some cases, sections appeared unremarkable except for luminal white blood cells or an occasional red blood cell (Fig. 2 a, b). In these sections, neurons appeared normal and only mild astrocytic swelling was seen. In contrast, other specimens contained numerous neurons with severe ischemic cell change (grade 2) associated with a vacuolated neuropil (Fig. 2 c, d). In these specimens, dark shrunken neurons were associated with swollen perivascular astrocytic endfeet. All animals had at least one region with dark, shrunken neurons with 1.7 ± 0.3 regions per animal having severely affected neurons. The medulla was the only region that did not contain neuronal injury in any of the six animals in this group. The number of areas having grade 2 neurons was higher in this group compared with either group 1 or 3, $P < 0.05$. Leukocytes, sometimes occurring in clusters were observed adhering to the endothelial lining of venules and capillaries. Leukocytes were present in 3.8 ± 0.6% of the vessels counted ($P < 0.05$ compared with group 1). In the most severely affected samples showing evidence of early infarction, the neuropil appeared pale and edematous with vacuolation (Fig. 2 d). In these areas, astrocytic cell bodies and perivascular processes were severely swollen. Dark neurons were occasionally associated with specific neuronal populations. For example, within the cerebellum Purkinje neurons appeared to be selectively vulnerable to early neuronal injury (Fig. 2e). In the hippocampus, granular neurons of the dentate gyrus and CA4 hippocampal pyramidal cells were commonly abnormal in appearance (Fig. 2f).

Ultrastructural examination also demonstrated a wide spectrum of abnormalities. Luminal mononuclear and polymorphonuclear (PMN) leukocytes were identified in venules and capillaries (Fig. 3 a, b). Leukocytes commonly contained pseudopodia which in some cases made contact with the endothelial surfaces (Fig. 3 a, c). At sites of leukocyte-endothelial adhesion, junctional complexes between the two cells were observed. Endothelial microvillus projections were also seen extending toward the luminal leukocyte (Fig. 3 c). Of all the vessels that con-

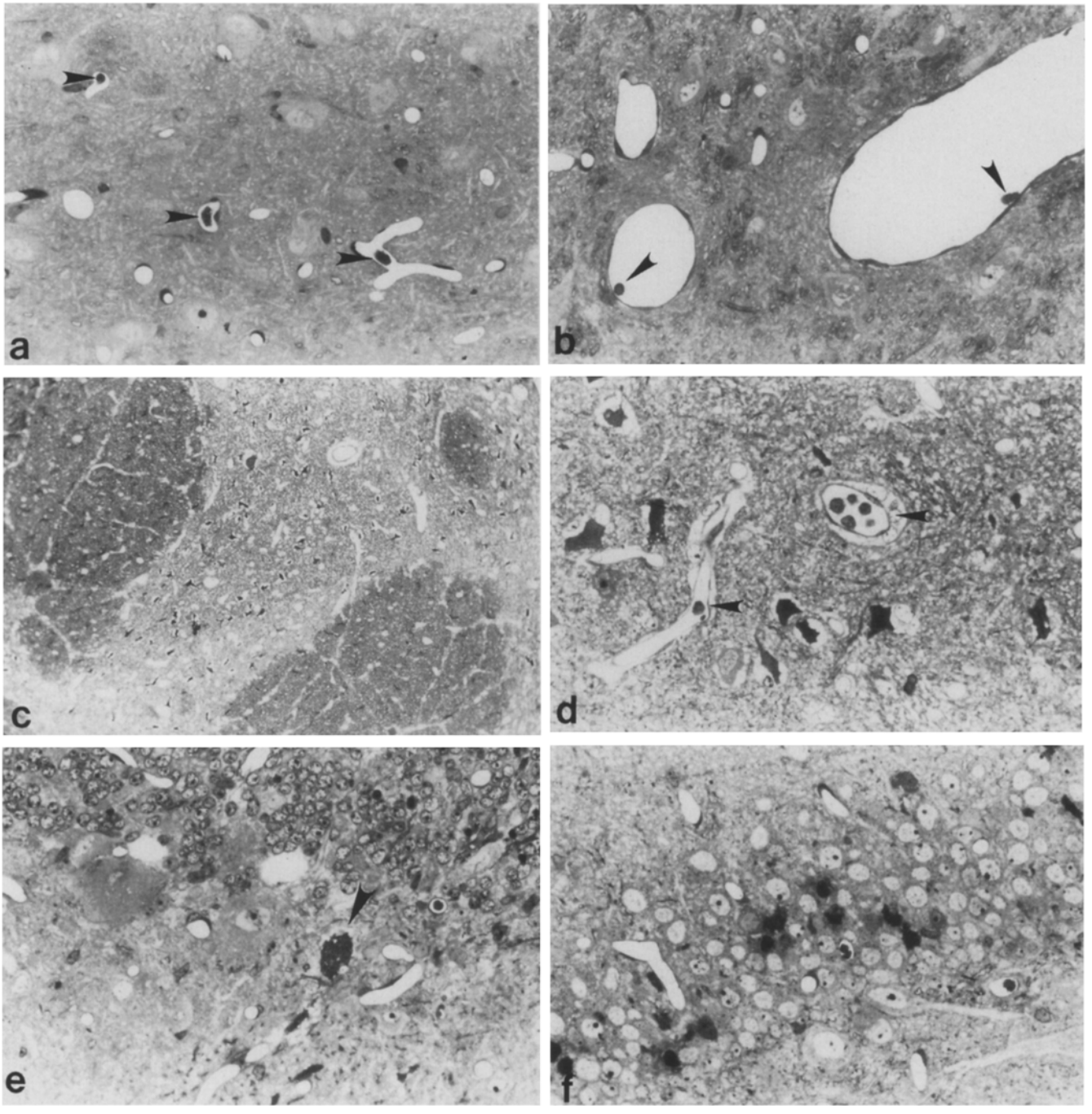

Fig. 2a–f Toluidine-blue-stained plastic sections of piglet brains 4 h after cardiac arrest. **a** Luminal leukocytes (*arrowheads*) are present within brain stem microvessels. Note that the surrounding brain parenchyma appears normal. **b** Within the thalamus, adhering leukocytes are present within venules. (*arrowheads*). **c** Dark neurons are present within the caudate nucleus. **d** Dark shrunken cortical neurons are associated with microvessels containing leukocytes (*arrowheads*). Surrounding parenchyma is vacuolated and perivascular swelling is present. **e** A cerebellar Purkinje neuron (*arrowhead*) is dark and shrunken. **f** Within the dentate gyrus, dark granule cells are present. **a–f** × 800

tained leukocytes, 42% also had either endothelial blebs or perivascular astrocytic swelling. Given that only 3.8% of the vessels contained leukocytes and that 29% of the vessels were damaged, this is a highly significant finding.

Endothelial cells were frequently vacuolated and commonly contained plasma membrane blebs and discontinuities (Fig. 3 a, d). These changes occurred in arterioles, venules and capillaries. In this group, 13.1 ± 5.5% of vessel surfaces showed endothelial blebs. This wide variation was accounted for by two animals in which less than 3% of vessels contained endothelial blebs. Tight junctions appeared intact but surface folds were frequently seen. Perivascular astrocytic swelling was seen in 16.1 ± 7.1% of vessels in all brain regions. Two animals in this group had no evidence of perivascular swelling. One animal in

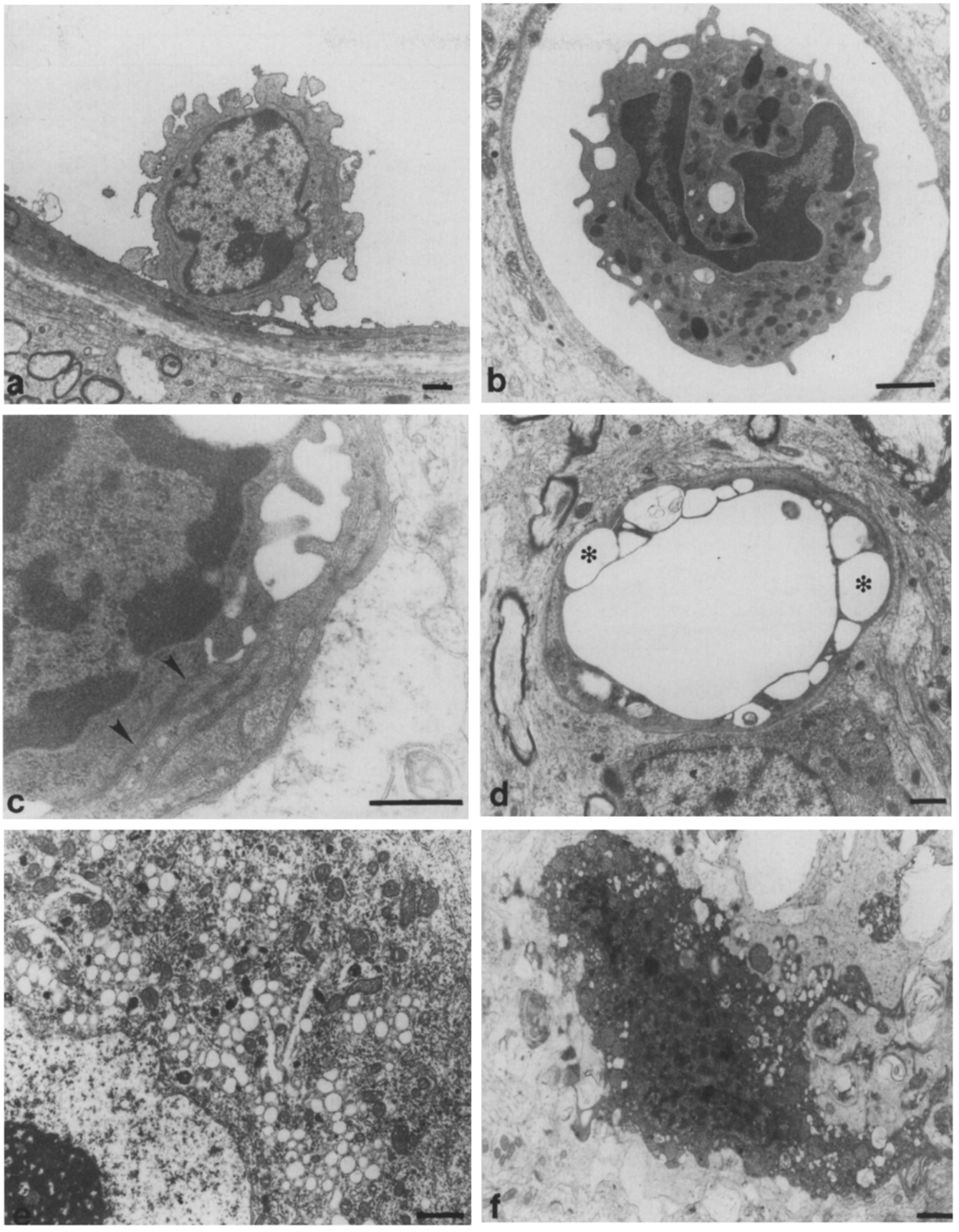

Fig. 3a–f Transmission electron micrographs of post-arrest piglet brains. **a** Adhering leukocyte that appears to be a monocyte is present within a cortical venule. The cell surface is irregular in contour. Note the site of membrane discontinuity on the intravascular endothelial surface. **b** Luminal polymorphonuclear leukocyte within caudate nucleus. **c** Leukocyte is shown adhering to vascular endothelium (*arrowheads*). Endothelial cell and leukocyte demonstrate pseudopodia and microvilli. **d** Numerous endothelial vacuoles (*asterisk*) are present within this cortical microvessel. Similar endothelial lesions were also observed in piglets from group 3. **e** Cortical neuron showing abnormally large numbers of perinuclear cytoplasmic vacuoles. **f** Dark shrunken neuron with pyknotic nucleus appears irreversibly injured. *Bars* **a, b, d–f** = 1 mM, **c** = 0.5 mM. **a** × 5,000; **b** × 9,700; **c** × 31,500; **d** × 6,300; **e** × 7,900; **f** × 6,300

Table 2 Vascular changes and leukocytes. All numbers represent the number of abnormal vessels or leukocytes as a percentage of total vessels counted. (*PVC* perivascular swelling, *CTX* cortex, *THA* thalamus, *HIP* hippocampus, *CAU* caudate nucleus, *MED* medulla, *CER* cerebellum)

	Group 1	Group 2	Group 3
Total vessels counted	371 ± 24	461 ± 40	459 ± 16
Total blebs	0.8 ± 0.5	13.1 ± 5.5	8.7 ± 1.8
Total PVC	0.6 ± 0.6	16.1 ± 7.1	4.3 ± 3.5
Total blebs and PVC	1.4 ± 0.6	29.2 ± 6.9*	13.0 ± 2.1*
Total WBC	1.4 ± 0.6	3.8 ± 0.6*	1.6 ± 0.6
Blebs			
CTX	1.6 ± 1.0	10.8 ± 7.7	12.5 ± 5.0*
THA	0.4 ± 0.4	10.8 ± 7.7	3.5 ± 1.8*
HIP	0.4 ± 0.4	14.7 ± 5.2*	10.0 ± 3.1*
CAU	0.9 ± 0.6	12.2 ± 4.3*	10.3 ± 1.7*
MED	0.7 ± 0.7	13.5 ± 5.9	6.2 ± 0.8*
CER	0.7 ± 0.4	14.4 ± 6.4	6.8 ± 2.8*
PVC			
CTX	1.7 ± 1.7	29.5 ± 15.9	3.7 ± 1.9
THA	0.4 ± 0.4	1.5 ± 0.8**	0
HIP	0.3 ± 0.3	27.5 ± 13.5	6.7 ± 5.5
CAU	1.1 ± 1.1	27.0 ± 17.1	16.7 ± 16.7
MED	0	0 ± 0**	0
CER	0	7.5 ± 4.9	0
WBC			
CTX	1.6 ± 0.8	5.9 ± 1.1*	1.3 ± 1.3
THA	0.4 ± 0.4	2.8 ± 0.7*	1.1 ± 0.6
HIP	0.6 ± 0.4	4.8 ± 1.8*	0
CAU	2.4 ± 1.0	4.1 ± 1.0	3.0 ± 1.6
MED	1.4 ± 0.4	2.5 ± 1.1	2.1 ± 0.9
CER	2.1 ± 0.9	3.0 ± 0.7	1.6 ± 1.0

* $P < 0.05$ compared with group 1
** $P < 0.05$ compared with cortex within group

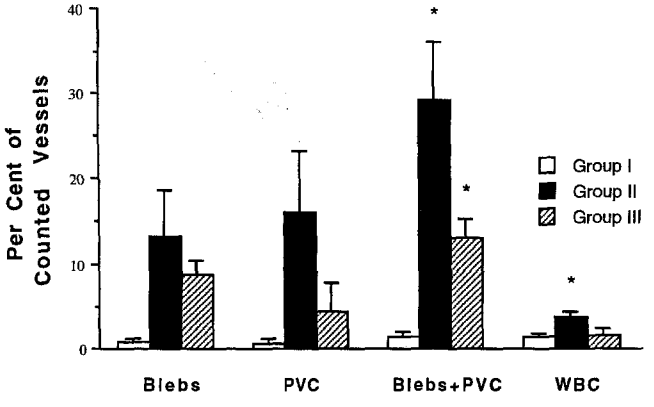

Fig. 4 Percentage of vessels counted for the three groups (see *key*) containing endothelial blebs, PVC, blebs plus PVC, or WBC. Data are shown as mean ± SEM, *$P < 0.05$ compared with group 1 (*PVC* perivascular swelling, *WBC* leukocytes with either blebs or perivascular swelling)

this group had neither perivascular swelling nor endothelial blebs. Although no regional differences in the incidence of endothelial blebs were seen within the ischemic group, thalamus and medulla had less perivascular swelling than did the cortex. A higher number of endothelial blebs were observed in the hippocampus and caudate nucleus compared with group 1. We calculated an endothelial injury severity score by adding the percentage of vessels containing either endothelial blebs or perivascular swelling (Fig. 4, Table 2). In this group 29.2 ± 6.9% of vessels contained an abnormality ($P < 0.05$ compared with time control).

The morphological changes in neurons were found to be heterogeneous. While the majority of neurons appeared normal, small populations of neurons showed moderate to severe ultrastructural changes. In the mildly affected neurons, large numbers of perinuclear cytoplasmic vacuoles were observed (Fig. 3e). In these neurons, other cytoplasmic organelles including mitochondria and Golgi bodies were normal. In the more severely injured neurons, the cytoplasm and nucleoplasm appeared electron dense, and cytoplasmic vacuoles were again present. Finally, the most severely affected neurons contained pyknotic nuclei, dark cytoplasm, cytoplasmic microvacuoles and dilated mitochondria (Fig. 3 f). Severely affected neurons were routinely surrounded by enlarged astrocytic processes. Astrocytic cell bodies were also moderately swollen.

Group 3 – Hypertensive controls

The severity of the endothelial injury, including membrane discontinuities, blebs, and perivascular swelling, was significantly higher than in time controls (13.0 ± 2.1% vs 1.42 ± 0.6%, $P < 0.05$). HRP was occasionally seen in endothelium but without parenchymal extravasation. However, the percentage was not different from that seen for group 2. The percentage of vessels containing leukocytes was not different from that of time controls, and severe neuronal injury was not seen in any animal.

Discussion

Our findings document the occurrence of widespread morphological and ultrastructural changes in cerebral endothelial cells, neurons, and glia only 4 h after cardiac arrest and CPR in infant piglets. The microvascular abnormalities correlate well with the previously reported increase in BBB permeability to α-aminoisobutyric acid (AIB) 4 h after cardiac arrest and CPR in this model [40]. The early pathological changes following cardiac arrest include: (1) severely damaged cerebral endothelium characterized by luminal blebs and membrane disruption, (2) perivascular swelling of astrocytic processes, (3) HRP within endothelial cells and extravasated into surrounding brain parenchyma, (4) PMN and mononuclear leukocytes within cerebral vessels in areas of endothelial damage, and (5) ischemic changes in neurons.

This model of global brain ischemia is a clinically appropriate, albeit a difficult experimental model. Blood flow to the brain and all other organs is zero during cardiac arrest induced by ventricular fibrillation [27]. This differs from other models of cerebral ischemia in which flow to organs other than the brain is typically maintained at normal or mildly reduced levels [19]. This is an important feature of this model because complete ischemia differs from incomplete ischemia in the degree of lactic acidosis and histopathological outcome [11, 38]. In addition, ischemia-induced alterations in extracerebral organ function may influence the ultimate central nervous system pathology that develops during reperfusion [11].

The pattern of neuronal vulnerability which we found in the piglet brain following cardiac arrest differs from that found after forebrain ischemia in rodents [35]. However, direct comparisons between early (hours) versus late (days) ischemic neuronal injury are problematic. In our study we are describing patterns of early neuronal injury that are consistent with the time course of the ischemic cell process reported in experimental studies and in human tissue [4, 5, 12]. The significance of the present neuronal findings is that they are widespread and not restricted to selectively vulnerable regions.

The most severe, widespread, and early histopathological consequence of cardiac arrest and resuscitation occurred in the vascular endothelium. Although results did not reach statistical significance due to the variability of bleb formation in group 2 (two animals had less than 3% of vessels with blebs), there were regional differences between the 8-min ischemic group and the time control group in the hippocampus and caudate nucleus. Endothelial bleb formation has been observed previously after global ischemia in rabbits [6], and rats [10]. It has been postulated that blebs can obstruct blood flow causing no reflow [1], although the blebs in the present study did not appear large enough to obstruct lumina. The "puff of smoke" appearance of disrupted endothelial membrane has been seen in post-ischemic brain [6] and kidney [44]. These membrane disruptions may be the result of lipid peroxidation during ischemia [30] or early reperfusion [9, 49]. Bleb formation might be an intermediate stage in the formation of endothelial microvilli [12]. Microvillus formation may contribute to post-ischemic hypoperfusion by serving as a nidus for the attachment of blood elements [10]. In support of this, we found red blood cell stasis and adherence of leukocytes in areas of endothelial damage and extravasated HRP.

The presence of perivascular swelling with surrounding vacuolated parenchyma most likely represents vasogenic edema which occurs following global ischemia in a variety of animal species [13, 22]. Mild HRP extravasation into diffuse brain areas in the present study is consistent with our previous finding of a modest elevation of the transfer coefficient of AIB 4 h after cardiac arrest in this model [40]. Although there were scattered areas of HRP extravasation into brain substance, most of the HRP was found within endothelial cells near the surface of the brain without opening of endothelial tight junctions. Taken together, these data support a transcellular mechanism of HRP transport across the BBB in this study. An increase in pinocytotic vesicles has been seen in brain endothelial cells following ischemia [12, 33], meningitis [37] and seizures [34]. We would expect to find more extensive HRP leakage after longer periods of ischemia or reperfusion [47]. While a large number of studies have examined the functional integrity of the BBB after global brain ischemia, very few have addressed its function following cardiac arrest and CPR in an infant model. Arai et al. [2] observed increased BBB permeability to Evans blue dye in 30% of adult dogs following CPR. Additionally, the timing of BBB disruption may be species or age specific. For example, in adult dogs undergoing the same cardiac arrest and CPR protocol as in this study, no change in BBB permeability was observed 4 h after the onset of reperfusion [41].

Most of the piglets in our study (five out of six) developed systemic hypertension soon after return of spontaneous circulation, during the period after ischemia when cerebral vessels are maximally dilated [15]. Hypertension causes endothelial injury even in the absence of ischemic injury [21] and may augment ischemia-reperfusion injury, particularly with respect to vascular endothelium [18]. In piglets rendered ischemic for only 10 s followed by 6 min of CPR (group 3) and which showed systemic hypertension, we found some of the ultrastructural changes seen in those animals rendered ischemic for 8 min, but no increase in luminal leukocytes. Endothelial blebs were commonly observed in group 3, with significance reached in cortex, hippocampus, caudate nucleus, and medulla compared with group 1. However, intraluminal leukocytes were infrequent and severe neuronal injury was not seen in group 3. Acute hypertension has been shown to cause microvillus and bleb formation of cerebral endothelium, and increased BBB permeability [8]. Thus, the combination of cerebral ischemia plus hypertension appears to be responsible for the microvascular abnormalities induced by CPR.

An important finding of our study was the presence of leukocytes only 4 h after the onset of reperfusion. We ob-

served intravascular leukocytes in 33 of the 36 brain regions counted in the animals in group 2. Leukocyte accumulation was not due to incomplete brain perfusion since we observed leukocytes in only 1.4% of the vessels in group 1 compared with almost 4% in the ischemia group. The transvascular infiltration of white cells into infarcted brain tissue has generally been regarded to be a relatively late phenomenon following reperfusion, usually occurring after 24 h or more [26]. More recent studies, however, have confirmed the early presence of intravascular leukocytes in cerebral vessels following focal [8, 17] and global [12] ischemia. The presence of leukocytes in microvessels is essential in implicating them in both early microvascular injury and post-ischemic blood flow alterations. Their presence in areas of endothelial injury suggests that they are involved in the pathogenesis of these changes, as seen in other organs after ischemic injury [46, 50]. However, in the non-ischemic hypertensive group, group 3, the number of vessels containing leukocytes was not different from that in the control group, yet endothelial abnormalities were significantly higher. This suggests that ischemia is required for leukocyte-endothelial cell interactions seen in this study. One proposed mechanism for this phenomenon is that ischemia results in an increased interaction between leukocytes and stimulated endothelial cells through the binding of the adhesive integrin complex CD11, CD18 of the leukocyte to the endothelial intercellular adhesion molecule-1 (ICAM-1) [3, 28, 31]. Our finding of pseudopodal projections by both white blood cells and endothelial cells directed towards each other provides physical evidence for endothelial-white cell adhesion and attachment. This may have an important functional role in transendothelial leukocyte passage as seen in vitro [25, 29] and in lung [43] and mesentery [48]. Microinfarcts associated with both endothelial changes and the presence of leukocytes reflects a "no reflow" phenomenon in these areas [45]. Leukocytes can reduce blood flow either by plugging vessels or by causing vasoconstriction through the release of superoxide which binds to nitric oxide [24]. Alternatively, the occurrence of microinfarcts in this model might be explained by variability in cerebral blood flow during CPR. Although we previously found that pre-arrest cerebral blood flow and metabolism were maintained during CPR when instituted immediately after the onset of ventricular fibrillation [39], regional cerebral blood flow has not been measured in this model after 8 min of cardiac arrest.

Our findings have important clinical ramifications for patients following cardiac arrest. An increase in BBB permeability may allow for entry of potent medications used during CPR into endothelial cells or into brain parenchyma which could then change vascular tone or have direct effects on brain tissue itself. Recently the use of high doses of epinephrine has been supported by the American Heart Association [16]; however, higher doses of epinephrine could be detrimental by causing focal vasoconstriction and worsening post-ischemic hypoperfusion (α-adrenergic effect), or increasing the cerebral metabolic rate at a time when cerebral blood flow is still limited (β-adrenergic effect) [15]. Additionally, our findings suggest that neuroprotective compounds do not have to enter brain parenchyma to be protective if they exert beneficial effects on endothelial cells. This may be the case with oxygen radical scavengers which have been shown to ameliorate BBB permeability after cardiac arrest [42], despite the fact that they have not been shown to cross the BBB [20]. Finally, the presence of leukocytes in areas of injury during this early reperfusion period should lead to their inclusion in the design of therapeutic strategies in neuroresuscitation.

In conclusion, this study is the first to show early, widespread cerebral vascular injury associated with intravascular leukocytes in a large animal model after cardiac arrest and CPR. These findings are important in that, as we hypothesized, hypertension plays a role in the development of endothelial cell injury, but without evidence for leukocyte accumulation. Early therapeutic interventions aimed at protecting the endothelium and attenuating leukocyte-endothelial interactions may be beneficial following cardiac arrest and CPR, especially in the setting of post-arrest hypertension. Knowledge of these early pathological changes may increase our understanding of the mechanisms of ischemia-reperfusion injury in infants and improve our resuscitative techniques, particularly during the early reperfusion period.

Acknowledgements The authors are grateful to Yuxia Han and Marcilia Halley for their excellent technical assistance and to Morayma Barreto for her help in preparing the manuscript. This work was supported in part by NS27127.

References

1. Ames A III, Wright RL, Kowada M, Thurston JM, Majno G (1968) Cerebral ischemia. II. The no-reflow phenomenon. Am J Pathol 52: 437–453
2. Arai T, Watanabe T, Nagaro T, Matsuo S (1981) Blood-brain barrier impairment after cardiac resuscitation. Crit Care Med 9: 444–448
3. Bowes MP, Zivin JA, Rothlein R (1993) Monoclonal antibody to the ICAM-1 adhesion site reduces neurological damage in a rabbit cerebral embolism stroke model. Exp Neurol 119: 215–219
4. Brierley JB, Brown AW, Meldrum BS (1971) The nature and time course of the neuronal alterations resulting from oligemia and hypoglycemia in the brain of *Macaca mulatta*. Brain Res 25: 483–499
5. Brown AW (1977) Structural abnormalities in neurons. J Clin Pathol 30 [Suppl 11]: 155–169
6. Chiang J, Kowada M, Ames A III, Wright RL, Majno G (1968) Cerebral ischemia. III. Vascular changes. J Neurosurg 52: 455–465
7. Dean JM, Koehler RC, Schleien CL, Atchison D, Gervais H, Berkowitz I, Traystman RJ (1991) Improved blood flow during prolonged cardiopulmonary resuscitation with 30% duty cycle in infant pigs. Circulation 84: 896–904
8. Del Zoppo GJ, Schmid-Schonbein GW, Mori E, Copeland BR, Chang CM (1991) Polymorphonuclear leukocytes occlude capillaries following middle cerebral artery occlusion and reperfusion in baboons. Stroke 22: 1276–1283
9. Dietrich WD, Wei EP, Povlishock JT, Kontos HA (1980) Method for morphophysiological study of specific pial microvessels. Am J Physiol 238: H172–H175

10. Dietrich WD, Busto R, Ginsberg MD (1984) Cerebral endothelial microvilli: formation following global forebrain ischemia. J Neuropathol Exp Neurol 43: 72–83
11. Dietrich WD, Busto R, Yoshida S, Ginsberg MD (1987) Histopathological and hemodynamic consequences of complete versus incomplete ischemia in the rat. J Cereb Blood Flow Metab 7: 300–308
12. Dietrich WD, Halley M, Valdes I, Busto R (1991) Interrelationships between increased vascular permeability and acute neuronal damage following temperature-controlled brain ischemia in rats. Acta Neuropathol 81: 615–625
13. Dobbin J, Crockard HA, Ross-Russell R (1989) Transient blood-brain barrier permeability following profound temporary global ischemia: an experimental study using ^{14}C-AIB. J Cereb Blood Flow Metab 9: 71
14. Eisenberg MS, Bergner L, Hallstrom A (1980) Out-of-hospital cardiac arrest: improved survival with paramedic services. Lancet I: 812–815
15. Gervais HW, Schleien CL, Koehler RC, Berkowitz ID, Shaffner DH, Traystman RJ (1991) Effect of adrenergic drugs on cerebral blood flow, metabolism, and evoked potentials after delayed cardiopulmonary resuscitation in dogs. Stroke 22: 1554–1561
16. Guidelines for cardiopulmonary resuscitation and emergency cardiac care (1992) JAMA 268: 2172–2183
17. Hallenbeck JM, Dutka AJ, Tanishima T, Kochanek PM, Kumaroo KK, Thompson CB, Obrenovitch TP, Contreras TJ (1986) Polymorphonuclear leukocyte accumulation in brain regions with low blood flow during the early post-ischemic period. Stroke 17: 246–253
18. Hardebo JE, Beley A (1984) Influence of blood pressure on blood-brain barrier function in brain ischemia. Acta Neurol Scand 70: 356–359
19. Harris AP, Koehler RC, Gleason CA, Jones MD, Traystman RJ (1989) Cerebral and peripheral circulatory responses to intracranial hypertension in fetal sheep. Circ Res 64: 991–1000
20. Haun SE, Kirsch JR, Helfaer MA, Kubos KL, Traystman RJ (1991) Polyethylene glycol-conjugated superoxide dismutase fails to augment brain superoxide dismutase activity in piglets. Stroke 22: 655–659
21. Kontos HA, Wei EP, Dietrich WD, Navari RM, Povlishock JT, Ghatak NR, Ellis EF, Patterson JL Jr (1981) Mechanism of cerebral arteriolar abnormalities after acute hypertension. Am J Physiol 240: H511–H527
22. Kuroiwa T, Ting P, Martinez H, Klatzo I (1985) The biphasic opening of the blood-brain barrier to proteins following temporary middle cerebral artery occlusion. Acta Neuropathol (Berl) 68: 122–129
23. Lewis JK, Minter MG, Eshelman SJ, Witte MK (1983) Outcome of pediatric resuscitation. Ann Emerg Med 12: 297–299
24. Lipton SA, Choi YB, Pan ZH, Lei SZ, Chen HS, Sucher NJ, Loscalzo J, Singel DJ, Stamler JS (1993) A redox-based mechanism for the neuroprotective and neurodestructive effects of nitric oxide and related nitroso-compounds. Nature 364: 626–632
25. Marchesi V, Florey H (1960) Electron micrographic observations on the emigration of leukocytes. J Exp Physiol 45: 343–348
26. McCormick WF (1983) Vascular disease. In: Rosenberg RN (ed) The clinical neurosciences. Neuropathology. Churchill Livingstone, New York, p 66
27. Michael JR, Guerci AD, Koehler RC, Shi AY, Tsitlik J, Chandra N, Niedermeyer E, Rogers MC, Traystman RJ, Weisfeldt ML (1984) Mechanisms by which epinephrine augments cerebral and myocardial perfusion during cardiopulmonary resuscitation in dogs. Circulation 4: 822–835
28. Mori E, Del Zappo GJ, Chambers JD, Copeland BR, Arfors RE (1992) Inhibition of polymorphonuclear leukocyte adherence suppresses no-reflow after cerebral ischemia in baboons. Stroke 23: 712–718
29. Moser R, Schleiffenbaum B, Groscurth P, Fehr J (1988) Interleukin 1 and tumor necrosis factor stimulate human vascular endothelial cells to promote transendothelial neutrophil passage. J Clin Invest 83: 444–455
30. Nemoto EM, Shiu GK, Nemmer J, Bleyaert AL (1982) Attenuation of brain free fatty acid liberation during global ischemia: a model for screening potential therapies for efficacy? J Cereb Blood Flow Metab 2: 475–480
31. Okada Y, Copeland B, Mori E, Tung M-M, Thomas WS, Del Zappo GJ (1994) P-selectin and intercellular adhesion molecule expression after focal brain ischemia and reperfusion. Stroke 25: 202–211
32. Peters A, Palay SL, Webster H (1976) The fine structure of the nervous system. Saunders, Philadelphia, pp 11–65
33. Petito CK (1979) Early and late mechanisms of increased vascular permeability following experimental cerebral infarction. J Neuropathol Exp Neurol 38: 222–234
34. Petito CK, Schaefer JA, Plum F (1977) Ultrastructural characteristics of the brain and blood-brain barrier in experimental seizures. Brain Res 127: 251–267
35. Pulsinelli WA, Brierley JB, Plum F (1982) Temporal profile of neuronal damage in a model of transient forebrain ischemia. Ann Neurol 11: 491–498
36. Pulsinelli WA, Levy DE, Duffy TE (1982) Regional cerebral blood flow and glucose metabolism following transient forebrain ischemia. Ann Neurol 11: 500–509
37. Quagliarello VJ, Long WJ, Scheld WM (1986) Morphologic alterations of the blood-brain barrier with experimental meningitis in the rat: temporal sequence and role of encapsulation. J Clin Invest 77: 1084–1095
38. Rehncrona S, Mela L, Siesjo BK (1979) Recovery of brain mitochondrial function in the rat after complete and incomplete cerebral ischemia. Stroke 10: 437–446
39. Schleien CL, Dean JM, Koehler RC, Michael JR, Chantarojanasiri T, Traystman RJ, Rogers MC (1986) Effect of epinephrine on cerebral and myocardial perfusion in an infant animal preparation of cardiopulmonary resuscitation. Circulation 73: 809–817
40. Schleien CL, Koehler RC, Shaffner DH, Traystman RJ (1990) Blood-brain barrier integrity during cardiopulmonary resuscitation in dogs. Stroke 21: 1185–1191
41. Schleien CL, Koehler RC, Shaffner DH, Eberle B, Traystman RJ (1991) Blood-brain barrier disruption after cardiopulmonary resuscitation in immature swine. Stroke 22: 477–483
42. Schleien CL, Koehler RC, Shaffner DH, Eberle B, Traystman RJ (1994) Reduced blood-brain barrier permeability after cardiac arrest by conjugated superoxide dismutase and catalase in piglets. Stroke 25: 1830–1835
43. Shaw JO (1980) Leukocytes in chemotactic fragment-induced lung inflammation. Vascular emigration and alveolar surface migration. Am J Pathol 101: 283–302
44. Sheehan HL, Davis JD (1959) Renal ischemia with failed reflow. J Pathol Bacteriol 78: 105–120
45. Siesjo BK (1981) Cell damage in the brain: a speculative synthesis. J Cereb Blood Flow Metab 1: 155–185
46. Tate RM, Repine JE (1983) Neutrophils and the adult respiratory distress syndrome. Am Rev Respir Dis 128: 552–559
47. Todd NV, Picozzi P, Crockard HA, Ross-Russell RW (1986) Duration of ischemia influences the development and resolution of ischemic brain edema. Stroke 17: 466–471
48. Von Andrian UH, Hansell P, Chambers JD, Berger EM, Filho IT, Butcher EC, Arfors KE (1992) L-selection function is required for b_2-integrin-mediated neutrophil adhesion at physiological shear rates in vivo. Am J Physiol 263: H1034–H1044
49. Watson BD, Busto R, Goldberg WJ, Santiso M, Yoshida S, Ginsberg MD (1984) Lipid peroxidation in vivo induced by reversible global ischemia in rat brain. J Neurochem 42: 268–274
50. Wedmore CV, Williams TJ (1981) Control of vascular permeability by polymorphonuclear leukocytes in inflammation. Nature 289: 646–650